

Epoxy 기능화된 Acrylate 입자가 가소화된 PLA Blown Films의 물성에 미치는 영향

Ye Zhang^{***}, Yan Zhao^{***}, Hongwei Pan^{***}, Xianzhong Lang^{***}, Huili Yang^{**}, Huiliang Zhang^{*,†},
Huixuan Zhang^{***}, and Lisong Dong^{**}

^{*}Synthetic Resins and Special Fiber Engineering Research Center, Ministry of Education, Changchun University of Technology

^{**}Key Laboratory of Polymer Ecomaterials, Chinese Academy of Sciences, Changchun Institute of Applied Chemistry

(2015년 12월 9일 접수, 2016년 1월 21일 수정, 2016년 2월 6일 채택)

The Influence of Epoxy Functionalized Acrylate Particles on the Properties of Plasticized PLA Blown Films

Ye Zhang^{***}, Yan Zhao^{***}, Hongwei Pan^{***}, Xianzhong Lang^{***}, Huili Yang^{**}, Huiliang Zhang^{*,†},
Huixuan Zhang^{***}, and Lisong Dong^{**}

^{*}Synthetic Resins and Special Fiber Engineering Research Center, Ministry of Education,
Changchun University of Technology, Changchun 130012, China

^{**}Key Laboratory of Polymer Ecomaterials, Chinese Academy of Sciences,
Changchun Institute of Applied Chemistry, Changchun, 130022, China

(Received December 9, 2015; Revised January 21, 2016; Accepted February 6, 2016)

Abstract: Polylactide (PLA) was plasticized with poly(diethylene glycol adipate) (PDEGA). The plasticized PLA was further blended with core-shell structured particles of glycidyl methacrylate-functionalized methyl methacrylate-butyl acrylate copolymer (GACR) using a twin-screw extruder, and the extruded samples were blown using the blown thin film technique. Both PDEGA and GACR significantly influenced the physical properties of the films. Compared to neat PLA, the elongation at break and tear strength of the films were significantly improved. The shear yielding induced by cavitation of GACR particles was the major tearing mechanism. GACR could act as a tear resistance modifier for PLA blown films. The spherulite size of the PLA/PDEGA/GACR films decreased with the addition of GACR. The biodegradability of the PLA/PDEGA/GACR films decreased slightly. These findings contributed new knowledge to the additive area and gave important implications for designing and manufacturing polymer packaging materials.

Keywords: polylactide, blown film, epoxy-functionalized acrylic impact modifier, mechanical properties, enzymatic degradation.

Introduction

In recent years, the serious problems of environmental pollution and fossil energy depletion have made an urgent need to develop renewable materials. So it's becoming prevalent that the traditional petroleum plastics have been substituted by biodegradable and renewable materials, known as "green materials".¹⁻³ Polylactide (PLA), a linear aliphatic polyester, is one of the most promising materials, which exhibits many advan-

tages, such as low toxicity, biocompatibility, renewability, energy saving and inherent biodegradability. PLA has established major applications such as packaging, paper coating, fibers, films, textile and disposable products.⁴⁻⁸ However, the inherent defects of PLA such as poor shock resistance, hard, brittleness, low thermal stability, high combustibility have significantly restricted its wide application.⁹ Therefore, much effort has been made to enhance these properties including chemical or physical method.^{10,11}

The common simple and more economic way to modify PLA is physical blending. Much attention has been pay to the blends of PLA with various materials including inorganic substances,¹² plasticizer, modifier and other polymers. Plasticizers

[†]To whom correspondence should be addressed.

E-mail: hlzhang@ciac.jl.cn

©2016 The Polymer Society of Korea. All rights reserved.

are widely used as additives for polymeric materials to enhance their flexibility, processability and ductility. Generally, an efficient plasticizer can decrease the modulus and tensile strength, as well as reduce glass transition temperature and melt temperature. Many types of plasticizers such as, poly(1,2-propylene glycol adipate) (PPA),¹³ poly(ethylene glycol) (PEG),¹⁴ and dioctyl phthalate (DOP)¹⁵ used to enhance the flexible properties of PLA have been investigated. Ljunberg¹⁶ proved that among five plasticizers triacetine and tributyl citrate are effective as plasticizers when blended with PLA. Poly(diethylene glycol adipate) (PDEGA) is a viscous liquid with a low T_g and can be prepared by diethylene glycol and adipic acid.¹⁷ It is a nontoxic biodegradable macromolecular plasticizer, which is eco-friendly to environment.¹⁸ With these advantages, it is a preeminent plasticizer to reinforce the flexibility and the processability of PLA film.

ACR(acrylic rubber) is a typically core-shell structured impact modifier, which contains poly(butyl acrylate) (PBA) as a rubbery core and poly(methyl methacrylate) (PMMA) as a glassy shell. It is usually used as a very effective impact modifier for polyvinyl chloride and PLA.¹⁹⁻²³ PMMA and PLA have similar polarity and solubility parameter ($\delta_{\text{PMMA}}=18.6$, $\delta_{\text{PLA}}=18.9$ ($\text{J}^{1/2} \text{ cm}^{3/2}$)),²⁴ so PMMA could effectively enhance the interfacial adhesion between the ACR particles and PLA matrix. However, simple blending of PLA with other components usually cannot produce very satisfactory properties. Reactive compatibilization is very often used to obtain blends with desirable properties because it can improve the miscibility and the interfacial adhesion of polymer blends. Glycidyl methacrylate (GMA)-grafted polymers are often used as compatibilizer for PLA blends. Oyama toughened PLA by reactive blending with poly(ethylene-glycidyl methacrylate) (EGMA).²⁵ The epoxy group of glycidyl methacrylate (GMA) can react *in situ* with the carboxyl and hydroxyl end groups of PLA during melt blending and can lead to an EGMA-grafted PLA copolymer that can compatibilize the blend. Other components containing GMA, such as glycidyl methacrylate grafted poly(ethylene octane) (POE-g-GMA),²⁶ styrene/acrylonitrile/glycidyl methacrylate copolymer (SANGMA),²⁷ ethylene/methyl acrylate/glycidyl methacrylate terpolymer,^{28,29} glycidyl methacrylate functionalized acrylonitrile-butadiene-styrene (ABS-g-GMA)³⁰ and butyl acrylate-ethyl acrylate-glycidyl methacrylate copolymer³¹ have been used to tough PLA. Recently, glycidyl methacrylate-functionalized methyl methacrylate-butyl acrylate (GACR) also has been studied to modify PLA by Li.³² It indicated that some interactions could take place between PLA

and GACR.

Up to now, no one has investigated that the application of GACR on polylactide blown film. In this work, we explored some properties of PLA/PDEGA/GACR blend film with various content of the reactive GACR, including thermal analysis, crystalline morphology, mechanical properties, and degradation behavior. In this studied system, GACR was prepared in an emulsion polymerization process. The new PLA/PDEGA/GACR films possess superior mechanical properties and degradation behavior, which are hopeful candidates for the application of daily life.

Experimental

Materials. PLA (4032D, melting-flow index of 1.64 g/min, a weight-average molecular weight (M_w) of 207000 g/mol, polydispersity index of 1.73, 2% D-LA) was supplied by Natureworks (U.S.A.) as a semi-crystalline grade. PDEGA was synthesized via polyesterification reaction using diethylene glycol and adipic acid as raw materials by our laboratory.¹⁸ In addition, tetra-*n*-butyl titanate and isooctanol were used as a catalyst and chain-ending reagent for the reaction, respectively. They were purchased from the Sinopharm Chemical Reagent Co., Ltd. It had weight-average molecular weight 19000 g/mol, the polydispersity index of 2.5, its viscous value was 12.4 Pa.s.

Synthesis of GACR and Preparation of the PLA/PDEGA/GACR Blend Films. GACR that had a core-shell ratio of 80/20 was synthesized by continuous polymerization according to Li wu's method as reported previously.³²

PLA and GACR were dried at 60 °C for 10 h in a vacuum oven. PLA/PDEGA/GACR blends were prepared by melt mixing with a vertical, corotating twin-screw extruder (SHJ-20, China, length/diameter ratio was 32:1, screw diameter was 20 mm, rotating speed was 150 rpm). The barrel temperature profile in different zones ranged from 160 to 190 °C. In addition, PDEGA was added through the lateral line feeder in the twin-screw extruder by measuring pump. The mixing components of PLA/PDEGA/GACR were 93/7/0, 89/7/4, 85/7/8, 81/7/12, and 77/7/16 w/w/w, respectively. After mixing all the samples were compression molded into sheets with thicknesses of 1.0 mm at 185 °C for dynamic mechanical analysis.

The PLA/PDEGA/GACR films were blown using a 30.0 mm smooth-bore single-screw extruder having an aspect ratio of 30:1 and fitted with a 46 mm diameter blown film die using external cooling air with temperature of 15 °C. The barrel tem-

perature profile in different zones ranged from 174 to 186 °C and the screw speed was kept at 38 rpm. Moreover, the extruder output was 8 kg/h, the blow up ratio (BUR) was 7, the frost line height (distance from die exit) was 15 cm and the winding speed was 7.0 m/min. The mechanical properties, thermal properties, morphology of the tear-fracture surfaces and degradation behavior of the blends or films were studied.

The Measurement of Latex Particle Size and the Properties of GACR. The particle size and distribution of PBA and GACR latex were characterized by Brookhaven 90-plus laser analyzer. The conversion rate of core component and shell component were calculated according to Li wu's method.³²

Thermal Analysis. Crystallization behavior of the composites was conducted under nitrogen flow by different scanning calorimetry (DSC) (TA Instruments DSC Q20 USA) on the specimens sliced from blown film samples. Film samples (7-9 mg) were heated from 0 to 190 °C at a rate of 10 °C/min and held at 190 °C for 3 min to erase the thermal history, then cooled at the same rate and finally heated again. The degree of crystallinity of the samples was evaluated from the heat evolved during fusion by the following relationship:

$$X_c = \frac{\Delta H_f}{w_{PLA} \times \Delta H_f^0} \times 100\% \quad (1)$$

where ΔH_f is the heat of fusion, ΔH_f^0 is the heat of fusion for 100% crystalline PLA (93 J/g)³³ and w_{PLA} is the weight fraction of PLA.

Dynamic Mechanical Analysis. Dynamic mechanical analysis (DMA) was carried out on a NETZSCH DMA 242C (Selb, Germany). The PLA/PDEGA/GACR blends were cut from the tensile bar specimens, which provided the plots of the storage modulus (E') and the dynamic loss factor ($\tan\delta$) against temperature. The samples were sized $W \times H \times L = 4 \times 1 \times 9 \text{ mm}^3$. The experiment was carried out in tension mode at a constant heating rate of 3 /min and a frequency of 1 Hz, from -70 to 150 °C.

Crystalline Morphology. An optical microscope (POM) (Olympus BX51) equipped with a temperature controller (Linkam THMS600) and a computer-controlled charged-coupled-device camera was used to investigate the crystalline morphology of pure PLA and PLA/PDEGA/GACR films. A small amount of sample with a thickness of approximately 0.025 mm was sandwiched between two microscope cover glasses and then placed on the hot stage. The samples were heated from room temperature to 190 °C at a rate of 30 °C/min, held there for 5 min to eliminate any previous thermal and

mechanical history, and then quenched to 110 °C at a rate of 30 °C/min for isothermal crystallization and held for 60 min. The morphology changes were recorded during the crystallization process.

Mechanical Behavior Testing. Uniaxial tensile tests were carried out at 23 ± 2 °C on an Instron 1121 testing machine (Canton, MA, USA). Specimens ($W \times H \times L = 20 \times 4 \times 0.025 \text{ mm}^3$) were cut from the previously blown films into a dumbbell shape in the machine direction (MD) and transverse direction (TD), respectively. The measurement was conducted at a cross-head speed of 50 mm/min at room temperature according to ASTM D882-2010. At least five runs for each sample were performed, and the results were averaged. Tensile strength, Young's modulus and elongation at break were obtained.

The right angle tearing strength was measured with an Instron 1121 testing machine. The cross-speed was set at 200 mm/min. The measurements were conducted according to QB/T1130-91 in the machine direction and transverse direction, respectively. At least five specimens were measured for each sample to get the average values.

Tear Fracture Surface of Films. The tear-fracture surfaces of PLA/PDEGA/GACR films were characterized with a scanning electron microscope (Model Japan JXA-840 ESEMFE). Then, samples were coated with a thin gold layer before to observe the morphology under high vacuum at 5 kV.

Enzymatic Degradation of Blown Films. The enzymatic degradation of the composites films was carried out in phosphate buffer (pH 8) containing *Pseudomonas mendocina* at 30 °C with shaking at 140 rpm. The composite films from the pressed sheets with thicknesses of 0.1 mm were chopped into square with gauge dimensions of $10 \times 10 \text{ mm}^2$. Then all samples were placed in small glass bottles containing the buffer and *P. mendocina*. The samples were picked up after a fixed time interval, washed with distilled water, and dried to constant weight in a vacuum, and then the weights of the films were measured. For comparison, neat PLA was treated with the same procedure.

Results and Discussion

Particle Size, Distribution and Properties of Latex. Figure 1 and 2 show the particle size distributions of PBA and GACR latexes, respectively. The dispersity of all latex was less than 0.1, so PBA and GACR latex were monodisperse. The particle size of PBA was increased from 108 to 124 nm after grafting copolymerization. The conversion rate of core com-

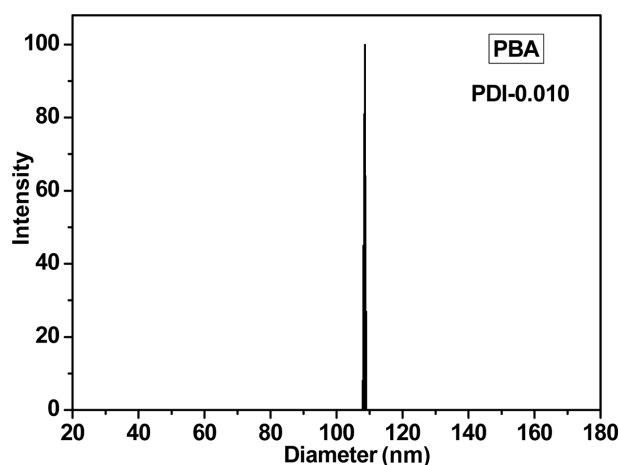


Figure 1. Particle size distribution of PBA.

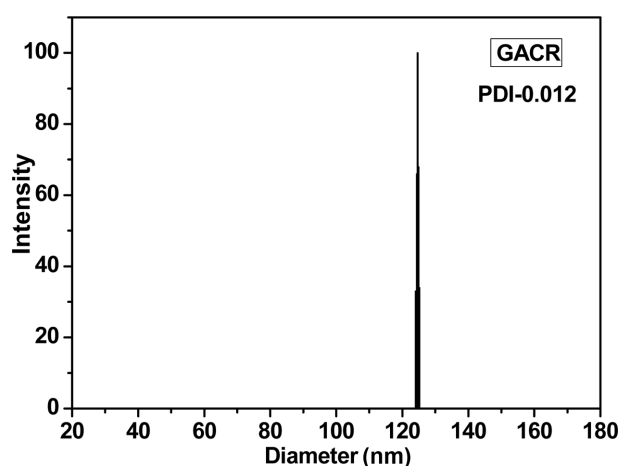


Figure 2. Particle size distribution of GACR.

ponent and shell component was listed in Table 1. The properties of GACR were listed in Table 2.

Thermal Properties. Figure 3 illustrates the DSC thermograms of PLA and all PLA/PDEGA/GACR films. In the thermograms, we observed three main transitions: glass transition, cold crystallization and melting transition. The various

Table 1. Conversion Rate of the Core and Shell Components

Designation	BA (%)	MMA and GMA (%)
Conversion rate	99.2	97.6

Table 2. Properties of GACR Latex

Designation	BA (wt%)	MMA (wt%)	GMA (wt%)	Particle size (nm)	Particle polydispersity
GACR	80.2	19.8	0.5	124	0.012

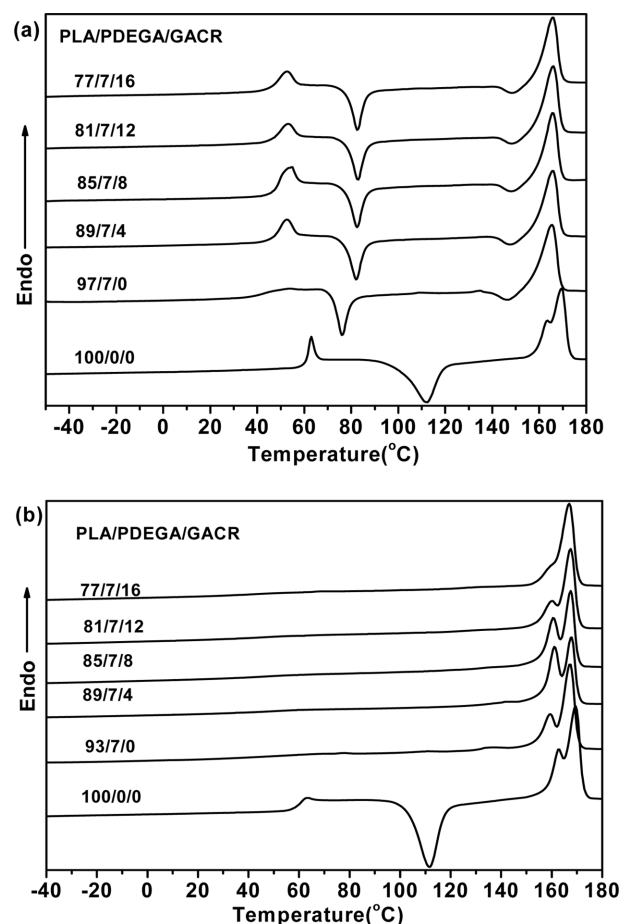


Figure 3. DSC thermograms of PLA/PDEGA/GACR films with compositions from 100/0/0 to 77/7/16: (a) the first heating run; (b) the second heating run.

DSC parameters are summarized in Table 3.

In the first heating run (Figure 3(a)), the glass transition temperature (T_g) of PLA/PDEGA decreased 18.7 °C compared with neat PLA and the cold crystallization temperature decreased significantly due to the incorporation of PDEGA. With the higher GACR content, there was no more decrease in T_g . The result indicated that PLA was incompatible with GACR particle. Neat PLA displayed a broad cold crystallization exotherm at approximately 112.0 °C. The incorporation of PDEGA decreased the cold crystallization temperature (T_{cc}) of neat PLA by approximately 35.9 °C. It indicated that PDEGA could be acted as a plasticizer for PLA. The T_{cc} of all

Table 3. Crystallization Properties of PLA/PDEGA/ACR Films

PLA/PDEGA/GACR (w/w/w)	T_g (°C)	T_{cc} (°C)	T_{m1} (°C)	T_{m2} (°C)	ΔH_f (J/g)	X_c (%)
First heating run						
100/0/0	61.8	112.0	163.5	169.6	43.5	46.8
93/7/0	43.1	76.1	-	165.4	40.8	47.2
89/7/4	50.1	82.1	-	165.7	37.9	45.8
85/7/8	49.8	82.5	-	165.7	34.7	43.9
81/7/12	49.6	82.8	-	165.9	32.9	43.7
77/7/16	49.8	82.6	-	165.7	31.3	43.4
Second heating run						
100/0/0	61.0	111.6	163.0	169.5	43.4	46.7
93/7/0	47.3	-	159.5	167.4	41.0	47.4
89/7/4	51.6	-	161.8	168.2	37.0	44.7
85/7/8	51.0	-	160.5	167.8	35.0	44.3
81/7/12	46.7	-	160.3	167.4	33.1	44.0
77/7/16	45.1	-	-	166.9	31.6	44.1

PLA/PDEGA/GACR was higher than that of PLA/PDEGA, but lower than that of PLA. It indicated that GACR had produced compatibilization reaction with PLA, there might exist covalent bonding at the blend interface. The compatibilization effect between PLA and GACR restricted the segmental mobility of PLA slightly. So the addition of GACR restricted the crystalline ability of PLA and decreased the rigidity of the PLA/PDEGA/GACR blend. The melting temperature of PLA/PDEGA and PLA/PDEGA/GACR film decreased about 4 °C compared with neat PLA.

From Figure 3(b), during the second heating run, all of the curves of the blends were changed greatly after the thermal history was eliminated. It could be seen that the peaks of glass transition of blends became not very apparent. The peaks of crystallization of blends were disappeared and it could not be seen. However, curve of the neat PLA was still nearly the same. It is possible that PDEGA increases the crystallization rate of PLA and these blends reach the maximum crystallization during the initial cooling procedure. Two melting endotherms were found in neat PLA and PLA/PDEGA/GACR blends in the DSC thermograms. This behavior is attributed to the formation of crystallites with different sizes and perfection which is arisen by lamellar rearrangement during crystallization.³⁴⁻³⁶ It can be noted that the size of the lower melting temperature peak decreased with increasing GACR content in the blend. This is possible that as the content of GACR increasing, the isolated GACR particles in the blend have

heavily agglomerated to form bigger particles, which limit the interactions between the carboxyl and hydroxyl end groups of PLA and the epoxy functional groups of GACR. As a result, this might have facilitated some of the less perfect crystals to melt and reorganize to more stable crystals and remelt at higher temperature. From the Table 3, in the first heating run and the second heating run, the crystallinity degree of the PLA/PDEGA/GACR films was slightly decreased with increasing GACR content.

Dynamic Mechanical Analysis. Figure 4 showed the dependence of storage modulus (E') and $\tan\delta$ on temperature for PLA/PDEGA blends modified with different contents of GACR. As shown in Figure 4(a), the addition of PDEGA and GACR decreased the storage modulus of neat PLA, and the E' of neat PLA gradually decreased with increasing temperature from -60 to 50 °C, then dropped rapidly because of the glass transition and finally reached a minimal value around 62 °C. The E' of the blends was lower than that of neat PLA between -45 and 60 °C and gradually decreased with increasing GACR content from -60 to 40 °C. This was attributed to the increasing content of GACR in the PLA/PDEGA/GACR blends, indicating a decreasing rigidity of the blends. On further increasing the temperature, a small peak could be seen around 83 °C. The peak was the characteristic peak of cold crystallization.³⁷ This cold crystallization process could also be detected by the DSC.

In Figure 4(b) and (c), neat PLA showed a single high temperature peak for T_g around 63 °C, PLA/PDEGA and PLA/

PDEGA/GACR4 blends showed a single peak for T_g (50 °C). While $\tan\delta$ curves revealed two glass transition peaks around -45 °C and 50 °C, with the higher T_g corresponding to PLA component, and the lower one to GACR component. When the content of GACR increased, the $\tan\delta$ peak corresponding to PLA component decreased. It suggested that PLA amorphous region was affected by the shell of GACR. There had taken place interaction at the blend interface. But the varied content of GACR did not result in an obvious change in the glass transition temperature, which was consistent with the result of DSC. Similar phenomenon had also been observed from the PLA/acrylate copolymer (ACR) blends and PLA/methyl methacrylate-butadiene-styrene (MBS) blends.^{20,37}

Crystalline Morphology. Figure 5 shows polarized microscope photographs of PLA/PDEGA/GACR films. Neat PLA spherulites appear as an obvious Maltese cross pattern in Fig-

ure 5(a). For the 93/7/0 PLA/PDEGA/GACR film, the size of PLA spherulites enlarges and the Maltese cross pattern becomes strong compared with neat PLA, which indicates that with the addition of PDEGA the molecular chain of PLA moves more easily and the crystallization rate of PLA increases. PDEGA leads to a perfect crystal structure of PLA (Figure 5(b)). For the 89/7/4, 85/7/8, 81/7/12, and 77/7/16 PLA/PDEGA/GACR films, GACR can be used as a heterogeneous nucleating agent of PLA, which causes the nucleating density of the spherulite to increase and the size of the spherulite to decrease (Figure 5(c)-(f)). The spherulite size of 100/0/0, 93/7/0, 89/7/4, 85/7/8, 81/7/12, and 77/7/16 films were approximately 103, 159, 65, 42, 34, and 23 μm , respectively. At the same time, because of compatibilization reactions between the carboxyl and hydroxyl of PLA and the epoxy functional groups of GACR, the amorphous phase increased and crystallized phase decreased. The Maltese cross pattern

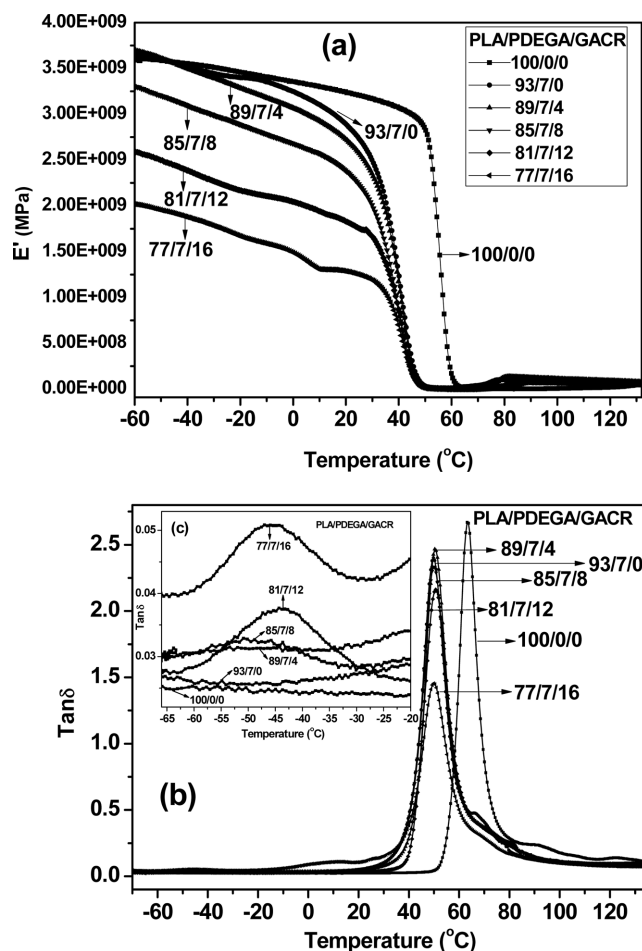


Figure 4. Dynamic mechanical properties of PLA/PDEGA/GACR blends: (a) the storage modulus (E'); (b) the loss factor ($\tan\delta$) (-70 ~135°C); (c) the loss factor ($\tan\delta$) (-65~-20 °C).

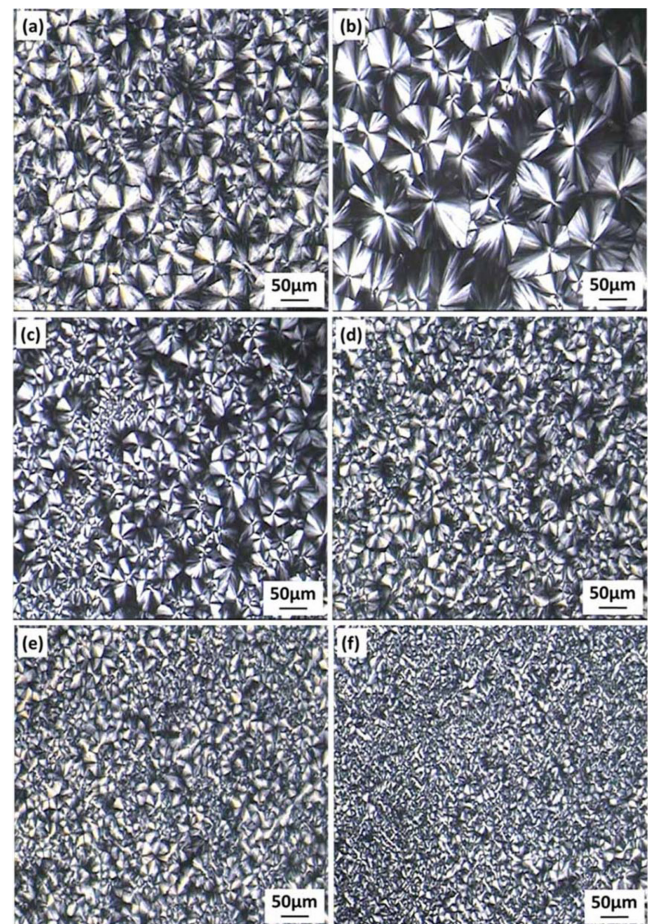


Figure 5. Spherulitic growth process of PLA/PDEGA/GACR blends at a crystallization temperature of 110 °C for 60 min: (a) 100/0/0; (b) 93/7/0; (c) 89/7/4; (d) 85/7/8; (e) 81/7/12; (f) 77/7/16.

phenomenon weakens and the spherulite size becomes smaller. The degree of crystallinity of films slightly reduced. This result was in consistent with the crystallinity data from DSC (Table 3).

Mechanical Properties. The tensile properties and tear strength of PLA/PDEGA/GACR films were given in Table 4. The addition of GACR improved the tensile behavior of the PLA and PLA/PDEGA films significantly, as was shown in Figure 6. The tensile strength of neat PLA film was 52.8 MPa (MD) and 54.0 MPa (TD), and the elongation at break was only about 10% (MD) and 7% (TD). The film showed brittle fracture upon tensile load. In contrast, all of the PLA/PDEGA/GACR films showed clear stress-strain curve yielding behavior upon stretching. After yielding occurred the strain developed continuously while the stress remained almost constant and the samples finally broke with a higher elongation at break than that of neat PLA. It was very interesting to find that the

77/7/16 PLA/PDEGA/GACR film had a high elongation at break of 87% and 69% in the machine direction and the transverse direction, respectively, while the tensile strength remained as high as 26.9 and 32.5 MPa.

Measuring the Young's modulus was the common method of determining the stiffness.³⁸ From Table 4, neat PLA film exhibited a modulus value of 2451 and 2323 MPa in the machine direction and the transverse direction, respectively. It was evident that the addition of PDEGA led to a decrease of the modulus value to 2120 and 2210 MPa, respectively. The addition of PDEGA decreased the T_g of PLA and improved its ductility and softness. The addition of GACR could further decrease the modulus of PLA/PDEGA/GACR films. When the content of GACR increased from 4% to 16%, the modulus decreased from 1890 and 1980 to 1140 and 1230 MPa in the machine direction and the transverse direction, respectively.

Table 4. Mechanical Properties of PLA/PDEGA/GACR Films

PLA/PDEGA/GACR (w/w/w)	Tensile strength MD/TD (MPa)	Elongation at break MD/TD (%)	Young's modulus MD/TD (MPa)	Tear strength MD/TD (K _N /m)
100/0/0	54.0±1.6/ 52.8±1.9	10±1.6/ 7±0.9	2451±153/ 2323±141	68±1.3/ 77±1.5
93/7/0	46.0±1.3/ 47.5±1.7	12±1.3/ 10±1.5	2120±146/ 2210±138	75±1.8/ 83±2.1
89/7/4	40.2±1.4/ 43.3±1.6	17±1.7/ 11±1.9	1890±126/ 1980±130	86±2.3/ 98±2.9
85/7/8	34.8±1.6/ 42.3±1.5	48±1.5/ 22±1.4	1720±114/ 1820±124	102±10.2/ 107±11.33
81/7/12	30.2±1.8/ 34.7±1.4	57±1.8/ 55±1.9	1520±132/ 1740±120	119±11.1/ 125±12.6
77/7/16	26.9±1.1/ 32.5±1.3	87±1.3/ 69±1.1	1140±117/ 1230±123	126±13.4/ 133±12.7

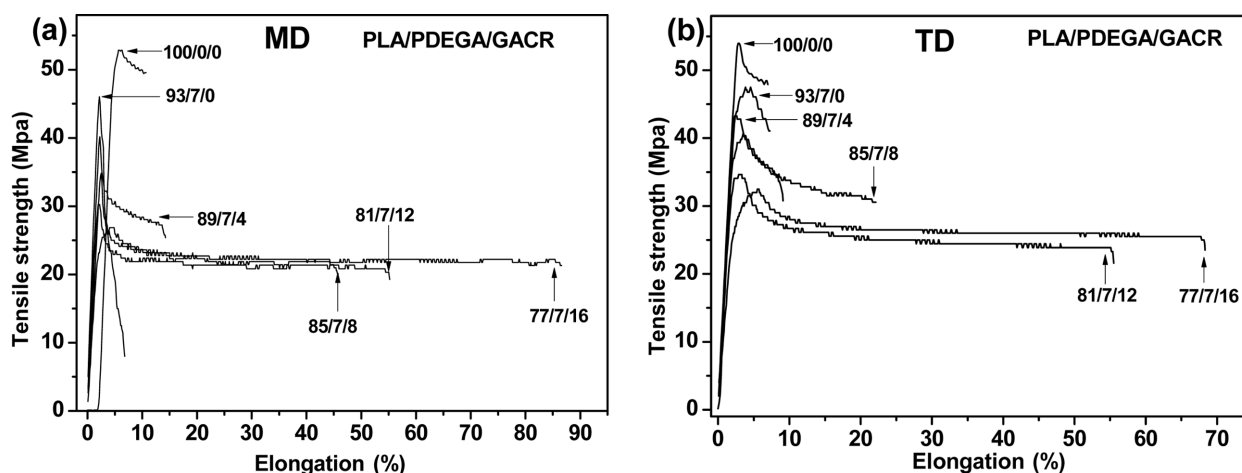


Figure 6. Tensile strength of PLA/PDEGA/GACR films: (a) machine direction (MD); (b) transverse direction (TD).

This indicated that GACR improved the flexibility of PLA/PDEGA/GACR blown films.

It was worth noting that the tear strength of the films had been improved in contrast with the tensile properties in Table 4. The neat PLA specimen exhibited relatively low tear strength values of 68 and 77 KN/m in the machine direction and the transverse direction, respectively. With increasing GACR content, the PLA/PDEGA/GACR films revealed a substantial increase in tear strength values. For the PLA/PDEGA/GACR blown films, when GACR content increased from 0 to 16 wt%, the tear strength values of PLA/PDEGA/GACR specimens in the machine direction and the transverse direction increased from 75 and 83 to 126 and 133 KN/m, respectively.

These research results indicated that the relatively poor tear strengths of the PLA could be significantly improved after melt blending with GACR. When GACR was introduced, the chemical entanglement due to reactive compatibilization and physical entanglement increased and then was conducive to enhancing the intermolecular force of the blends. For the PLA/PDEGA/GACR blown films, the good improvement of tensile strain at break and tear strengths might be ascribed to the intrinsic high flexibility of rubbery poly(butyl acrylate) core of GACR and the increased interaction of two components due to the reaction between carboxyl functional group of PLA and epoxy functional group of GACR. The tear strengths of the PLA/PDEGA/GACR films had been improved by absorbing the energy through deformation of the elastomer.

In addition, from the Table 4, elongation at break is higher along the machine direction relative to the transverse direction. Longitudinal Young's modulus is smaller than horizontal Young's modulus. However, during the right angle tearing strength process, the tearing strength of the film at the transverse direction was better than those at the longitudinal direction. On the whole, the machine direction had better mechanical properties than the transverse direction. This difference could be ascribed to that during the process of blown film, nip rolls produced traction for film and the film oriented at the machine direction. Thus, the PLA molecular chain was more easily to arrange in machine direction.

Surprisingly, the plasticizer and elastomer GACR in the PLA/PDEGA/GACR blown films has been found to yield a highly desired combination of high elongation at break, high tear strength and low Young's modulus required for most packaging applications. GACR could decrease the modulus of the blown films. The PLA/PDEGA/GACR blown films had excellent flexibility and mechanical properties.

Tear Fracture Surface of Films. SEM micrographs of the tearing fracture surface along the machine direction of PLA/PDEGA/GACR blown films are given in Figure 7. As shown in Figure 7(a)-(f), all blends films have a typical characteristic of a compatible structure. The fracture surfaces of 100/0/0 and 93/7/0 (Figure 7(a) and (b)) appear relatively smooth, indicating that little plastic deformation has taken place during the tearing test. This result is consistent with its lower elongation at break. From Figure 7(c) and (d), the tearing fracture surfaces of 89/7/4 and 85/7/8 PLA/PDEGA/GACR blown films exhibit rough and long stretches of ligaments, which suggests that the tear specimens have broken yieldingly. Some cavitations and a clear matrix deformation can be clearly identified for the PLA/PDEGA/GACR films. With the content of GACR increasing, cavities increase. These cavities are formed when the volumetric strain energy released by forming a void is greater than the surface energy needs to form a new surface plus the energy needs to stretch the surrounding rubber to make space for the void.³⁹ Especially, 81/7/12 and 77/7/16 PLA/PDEGA/GACR films display significantly ductile fracture on which rumpled surfaces can be seen (Figure 7(e) and (f)). The rumples lie parallel to the notch of highly drawn material. The occurrence of

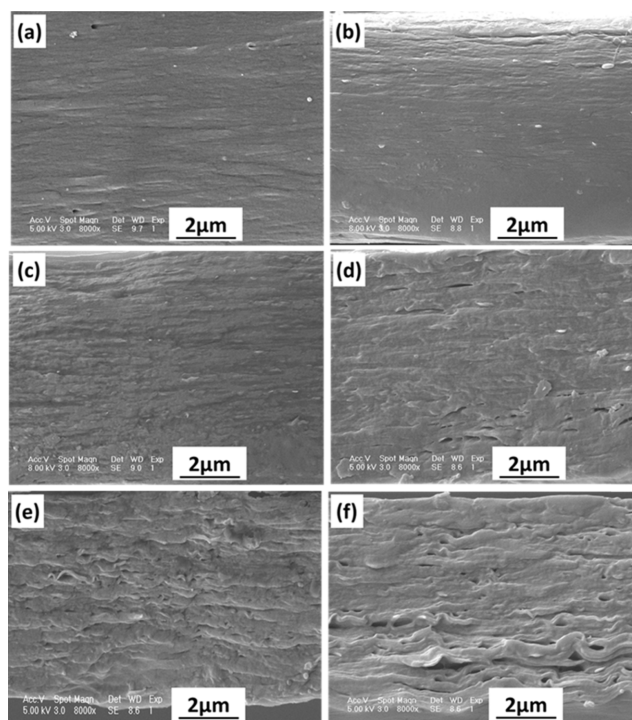


Figure 7. Images of the crack-tip damage zones of torn PLA/PDEGA/GACR blown films in the machine direction: (a) 100/0/0; (b) 93/7/0; (c) 89/7/4; (d) 85/7/8; (e) 81/7/12; (f) 77/7/16.

rumpled can be ascribed to the considerable tearing ahead of the crack tip before unstable fracture sets in. The extensive deformation ahead of the crack tip gives rise to these structures. In particular, extensive plastic deformation of the PLA matrix can be clearly observed, which implied that shear yielding of the PLA matrix has taken place. This is a typical feature of a ductile fracture. The occurrence of shear yielding induced by cavitation of GACR particles was the major tearing mechanism.

Enzymatic Degradation of Blown Films. PLA was the biodegradable materials. The biodegradability of PLA/PDEGA/GACR blown films was extremely important for the potential application of the materials in future. Here, enzymatic degradation tests were used to evaluate the biodegradability of the composites. *P. mendocina* which could produce lipase was used to degrade the PLA and its composites. Figure 8 showed the weight loss profiles of neat PLA and PLA/PDEGA/GACR blown films as a function of time during the enzymatic degradation. The weight losses of the films increased with time for all samples. The rate of enzymatic degradation could be determined from the slope of the weight loss against time.

At the first stage, the rates of enzymatic degradation for all the samples were slow, because there was an incubation period for the *P. mendocina*. It became faster after 1 day for neat PLA and PLA/PDEGA/GACR blown films. However, the rate of enzymatic degradation decreased with the addition of PDEGA compared with neat PLA. The influence of GACR content on the rate of enzymatic degradation depended on the time region. From the next day to the fourth day, the rate of enzymatic degradation increased with the addition of GACR. It was possible

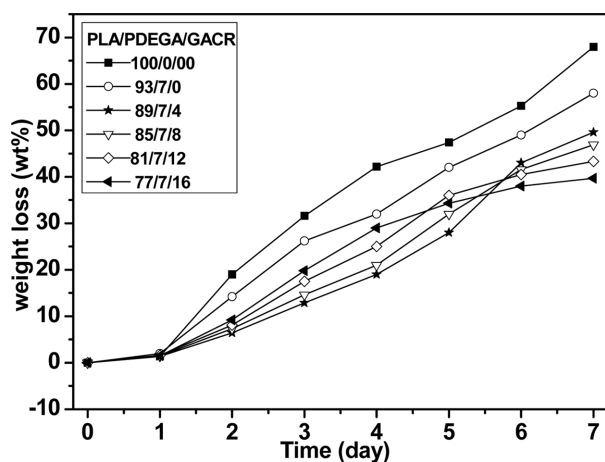


Figure 8. Weight loss profiles of neat PLA and PLA/PDEGA/GACR blown films as a function of time during the enzymatic degradation.

that decreasing of the size of the spherulites and the reducing of degree of crystallinity were the main influencing factors. On the fifth day, when enzymatic degradation achieved a certain degree, the rate of enzymatic degradation decreased with the addition of GACR. The reactions between the carboxyl and hydroxyl of PLA and the epoxy of functional groups of GACR limited the movement of molecular chain and entangled molecular chain shielded the diffusion of enzyme from the surface to the inside. Consequently, the enzymatic degradation of PLA was restrained. The final weight losses decreased with the increasing of GACR.

Conclusions

In this study, the PLA/PDEGA/GACR films have been prepared by a melt blending and extrusion blow film process. From the thermal and dynamic mechanical analysis, it was found that PDEGA could plasticize PLA and enhance the flexibility of PLA/PDEGA/GACR films. The elongation at break as well as the tear strength of PLA/PDEGA/GACR films was improved significantly compared with neat PLA. The tear strengths of the 77/7/16 PLA/PDEGA/GACR film in the machine direction and transverse direction were about 1.85 and 1.73 times that of neat PLA film, respectively. It was proved that the PLA/PDEGA/GACR blown films were high tearing resistance films. Moreover, from the SEM of tear fractured surfaces, while the content of GACR increased up to 12% and 16%, the large plastic deformation of PLA/PDEGA/GACR films appeared. This phenomenon indicated that the tear strength of PLA/PDEGA/GACR films was improved. GACR could be used effectively as a tear resistance modifier of PLA films. The biodegradability of the PLA/PDEGA/GACR films decreased slightly.

Acknowledgements: This work was supported by the fund of Chinese Science Academy (Changchun Branch) (No. 2014SYHZ0019), Development and Reform commission of Jilin Province of China (2015Y027), Science & Technology Bureau of Changchun City of China (2013279), and the National Science Foundation of China (51021003).

References

1. A. K. Mohanty, M. Misra, and G. Hinrichsen, *Macromol. Mater. Eng.*, **1**, 276 (2000).
2. T. U. Gerngross and S. C. Slater, *Sci. Am.*, **283**, 36 (2000).

3. M. V. Podzorovaa, Yu. V. Tertyshnayab, and A. A. Popova, *Russ. J. Phys. Chem. B*, **8**, 726 (2014).
4. A. J. Svagan, A. Akesson, M. Cardenas, S. Bulut, J. C. Knudsen, J. Risbo, and D. Plackett, *Biomacromolecules*, **13**, 397 (2012).
5. M. Omura, T. Tsukegi, Y. Shirai, H. Nishida, and T. Endo, *Ind. Eng. Chem. Res.*, **45**, 2949 (2006).
6. C. Reti, M. Casetta, S. Duquesne, S. Bourbigot, and R. Delobel, *Polym. Adv. Technol.*, **19**, 628 (2008).
7. S. W. Chun, S. H. Kim, Y. H. Kim, and H. J. Kang, *Polym. Korea*, **24**, 656 (2000).
8. G. H. Lee, S. J. Lee, S. W. Jeong, H. C. Kim, J. H. Choi, and S. G. Lee, *Polym. Korea*, **39**, 934 (2015).
9. A. J. Nijenhuis, E. Colstee, D. W. Grijpma, and A. J. Pennings, *Polymer*, **37**, 5849 (1996).
10. G. Bibi, Y. Jung, J. C. Lim, and S. H. Kim, *Polym. Korea*, **39**, 453 (2015).
11. W. Y. Jang, K. H. Hong, B. H. Cho, S. H. Jang, S. I. Lee, B. S. Kim, and B. Y. Shin, *Polym. Korea*, **32**, 116 (2008).
12. J. Kang, J. H. Lim, M. J. Moon, W. K. Lee, M. R. Kim, and J. K. Lee, *Polym. Korea*, **33**, 13 (2009).
13. H. L. Zhang, J. F. Fang, H. H. Ge, L. J. Han, X. M. Wang, Y. Y. Hao, C. Y. Han, and L. S. Dong, *Polym. Eng. Sci.*, **53**, 112 (2013).
14. F. Hassouna, J. M. Raquez, F. Addiego, P. Dubois, V. Toniazzo, and D. Ruch, *Eur. Polym. J.*, **47**, 2134 (2011).
15. S. L. Yang, Z. H. Wu, B. Meng, and W. Yang, *J. Polym. Sci., Part B: Polym. Phys.*, **47**, 1136 (2009).
16. N. Ljungberg and B. Wesslén, *J. Appl. Polym. Sci.*, **86**, 1227 (2002).
17. X. F. Wu, J. B. Zhao, and W. T. Yang, *J. Beijing Univ. Chem. Technol.*, **28**, 23 (2001).
18. H. Y. Liang, Y. P. Hao, S. R. Liu, H. L. Zhang, Y. S. Li, L. S. Dong, and H. X. Zhang, *Polym. Bull.*, **70**, 3487 (2013).
19. H. Y. Jiang, B. J. Liu, Y. J. Deng, J. Y. Ma, C. L. Cao, and H. X. Zhang, *Polym. Advan. Technol.*, **26**, 182 (2014).
20. H. Y. Liang, Y. P. Hao, J. J. Bian, H. L. Zhang, L. S. Dong, and H. X. Zhang, *Polym. Eng. Sci.*, **55**, 386 (2015).
21. X. G. Ge, S. George, S. Law, and M. Sain, *J. Macromol. Sci. B*, **50**, 2070 (2011).
22. X. L. Song, Y. Chen, Y. Z. Xu, and C. P. Wang, *Bioresources*, **9**, 1939 (2014).
23. Y. Fan, H. L. Zhang, G. F. Wu, and H. X. Zhang, *Polym. Korea*, **39**, 852 (2015).
24. G. B. Zhang, J. M. Zhang, S. G. Wang, and D. Y. Shen, *J. Polym. Sci., Part B: Polym. Phys.*, **41**, 23 (2003).
25. H. I. Oyama, *Polymer*, **50**, 747 (2009).
26. Y. Zhao, X. Z. Lang, H. W. Pan, Y. J. Wang, H. L. Yang, H. L. Zhang, H. X. Zhang, and L. S. Dong, *Polym. Eng. Sci.*, **55**, 2801 (2015).
27. Y. J. Li, and H. Shimizu, *Eur. Polym. J.*, **45**, 738 (2009).
28. X. Zhang, Y. Li, L. J. Han, C. Y. Han, K. Xu, C. Zhou, M. Y. Zhang, and L. S. Dong, *Polym. Eng. Sci.*, **53**, 2498 (2013).
29. G. F. Brito, P. Agrawal, E. M. Araujo, and T. J. A. de Melo, *Polimeros.*, **22**, 164 (2012).
30. S. L. Sun, M. Y. Zhang, H. X. Zhang, and X. M. Zhang, *J. Appl. Polym. Sci.*, **122**, 2992 (2011).
31. Y. P. Hao, H. H. Ge, L. J. Han, H. L. Zhang, L. S. Dong, and S. L. Sun, *Chinese J. Polym. Sci.*, **31**, 1519 (2013).
32. W. Li, D. D. Wu, S. L. Sun, G. F. Wu, H. X. Zhang, Y. J. Deng, H. L. Zhang, and L. S. Dong, *Polym. Bull.*, **71**, 2881 (2014).
33. E. W. Fischer, H. J. Sterzed, and G. Wegner, *Colloid Polym. Sci.*, **251**, 980 (1973).
34. A. J. Nijenhuis, E. Colstee, D. W. Grijpma, and A. J. Pennings, *Polymer*, **37**, 5849 (1996).
35. E. Piorkowska, E. Kulinski, A. Galeski, and R. Masirek, *Polymer*, **47**, 7178 (2006).
36. F. Ali, Y. W. Chang, S. C. Kang, and J. Y. Yoon, *Polym. Bull.*, **62**, 91 (2009).
37. H. L. Zhang, N.A. Liu, X. H. Ran, C. Y. Han, L. J. Han, Y. G. Zhuang, and L. S. Dong, *J. Appl. Polym. Sci.*, **125**, 550 (2012).
38. V. L. Finkenstadt, C. K. Liu, P. H. Cooke, L. S. Liu, and J. L. Willett, *J. Polym. Environ.*, **16**, 19 (2008).
39. A. Lazzeri and C. B. Bucknall, *J. Mater. Sci.*, **28**, 6799 (1993).